### Title

Rapid Chagas Disease Drug Target Discovery Using Directed Evolution in Drug-Sensitive Yeast




### Journal

ACS Chemical Biology, 12(2)

### ISSN

1554-8929



### Authors

Ottilie, Sabine
Goldgof, Gregory M
Calvet, Claudia Magalhaes
et al.



### Publication Date

2017-02-17

### DOI

10.1021/acschembio.6b01037

Peer reviewed

HHS Public Access

Author manuscript

*ACS Chem Biol*. Author manuscript; available in PMC 2017 October 20.

Published in final edited form as:

*ACS Chem Biol*. 2017 February 17; 12(2): 422–434. doi:10.1021/acschembio.6b01037.

# Rapid Chagas disease drug target discovery using directed evolution in drug-sensitive yeast

**Sabine Ottilie**[1,8], **Gregory M. Goldgof**[1,5,8], **Claudia Magalhaes Calvet**[3,6], **Gareth K. Jennings**[3], **Greg LaMonte**[1], **Jake Schenken**[1], **Edgar Vigil**[1], **Prianka Kumar**[1], **Laura-Isobel McCall**[3], **Eduardo Soares Constantino Lopes**[1,4], **Felicia Gunawan**[1], **Jennifer Yang**[1], **Yo Suzuki**[5], **Jair L. Siqueira-Neto**[3], **James H. McKerrow**[3], **Rommie E. Amaro**[2], **Larissa M. Podust**[3], **Jacob D. Durrant**[2,7], and **Elizabeth A. Winzeler**[1]

[1]Department of Pediatrics, University of California, San Diego, School of Medicine, La Jolla, California 92093, USA

[2]Department of Chemistry & Biochemistry, University of California, San Diego, La Jolla, California 92093-0340, United States

[3]Skaggs School of Pharmacy and Pharmaceutical Sciences, University of California San Diego, La Jolla, California 92093, USA

[4]Department of Pharmacy, Federal University of Paraná, Curitiba, PR, Brazil (80210-170)

[5]Department of Synthetic Biology and Bioenergy, J. Craig Venter Institute, La Jolla, California 92037, USA

[6]Cellular Ultrastructure Laboratory, IOC, FIOCRUZ, Rio de Janeiro, RJ, Brazil (21045-360)

## Abstract

Recent advances in cell-based, high-throughput phenotypic screening have identified new chemical compounds that are active against eukaryotic pathogens. A challenge to their future development lies in identifying these compounds' molecular targets and binding modes. In particular, subsequent structure-based chemical optimization and target-based screening require a detailed understanding of the binding event. Here we use directed evolution and whole-genome sequencing of a drug-sensitive *S. cerevisiae* strain to identify the yeast ortholog of *Tc*Cyp51,

[7]Current address: Department of Biological Sciences, University of Pittsburgh, Pittsburgh, Pennsylvania, 15260, United States

[8]These two authors contributed equally to this work.

Supporting Information

Sequences have been placed in the short read sequence archive (http://www.ncbi.nlm.nih.gov/sra) under accession code PRJNA313356 for ABC16 and PRJNA320899 for mutant lineages

**Author Contributions**

S.O., G.M.G., L.P., J.D.D., and E.A.W. designed the experiments and wrote the manuscript. Directed-evolution experiments were designed and performed by Y.S., G.M.G., and E.V. Yeast $IC_{50}$ experiments were performed by S.O., G.M.G., E.V., J.Y., P.K. and J.S.. $IC_{50}$ experiments in parasites were designed and performed by J.L.D.S.N., G.L., L.I.M., and J.H.M. Cyp51 inhibition studies were done by S.O. and G.K.J., and C.C.A. performed GC-MS experiments. Whole-genome sequencing was performed by the UCSD Institute for Genomic Medicine Core Facility. Sequence analysis was performed by G.M.G. and F.G. Computational docking studies were designed and performed by J.D.D. and R.E.A. Crystallography experiments were performed, designed, and conducted by L.P. and E.S.C.L.

**Conflict of Interest**

REA is a co-founder of Actavalon, Inc. The authors otherwise declare that they have no competing financial interests.

lanosterol-14-alpha-demethylase (*Tc*Cyp51), as the target of MMV001239, a benzamide compound with activity against *Trypanosoma cruzi*, the etiological agent of Chagas disease. We show that parasites treated with MMV0001239 phenocopy parasites treated with another *Tc*Cyp51 inhibitor, posaconazole, accumulating both lanosterol and eburicol. Direct drug-protein binding of MMV0001239 was confirmed through spectrophotometric binding assays and X-ray crystallography, revealing a binding site shared with other anti-trypanosomal compounds that target Cyp51. These studies provide a new probe chemotype for *Tc*Cyp51 inhibition.

### Keywords

Chagas disease; *T. cruzi*; ergosterol; Cyp51; *ERG11*; *S. cerevisiae*; directed evolution; whole genome sequencing

## Introduction

Chagas disease, the deadliest parasitic illness endemic to Latin America, is caused by infection with the unicellular parasite *Trypanosoma cruzi*. Though prevalent in Latin America, it has recently emerged in North America and Europe as well. Global costs associated with the condition are estimated at 7 to 19 billion US dollars per year.[1]

The disease manifests itself in both acute and chronic phases. The initial acute or asymptomatic phase lasts a few weeks as parasites multiply in tissues and organs.[2] If present, symptoms are usually mild, but occasionally life-threatening myocarditis or meningoencephalitis can occur, leading to death in about ten percent of infected individuals. Ten to thirty percent of infected survivors subsequently develop chronic Chagas disease, with symptoms that only manifest after years or decades. The chronic form can cause tissue and organ damage, with potentially lethal complications from cardiomyopathy.[2]

Currently, only two drugs, benznidazole and nifurtimox, are available, but both have variable efficacy and are known to induce adverse neurological and gastrointestinal drug reactions.[3] Furthermore, the recent BENEFIT (Benznidazole Evaluation for Interrupting Trypanosomiasis) clinical trial demonstrated that benznidazole is ineffective in symptomatic chronic-stage patients.[4–6] Safer, more effective drugs are needed to treat both the chronic and acute stages, especially in vulnerable patients such as children and pregnant women.[7]

One approach for discovering new active leads is to perform phenotypic screens, which in recent years have identified an ever-increasing number of anti-trypanosomal compounds.[8] In most cases, the targets of these compounds are not known. When a tool compound has undesirable activities or low potency, target discovery can provide new approaches that inform the drug-development process. In addition, mapping compounds to targets can yield useful chemical tools for perturbing specific pathways and studying parasite biology.

Recently we have shown that the surrogate species *S. cerevisiae*, which has a well-characterized, small haploid genome, can be used to discover the target of drug candidates or phenotypic-screening hits discovered in another eukaryotic pathogen, *P. falciparum*. For example, cladosporin targets lysl-tRNA synthetase in both *Saccharomyces* and *P.*

*falciparum*.[9] In addition, directed evolution in yeast showed that that the spiroindolone antimalarial KAE609, which is a P-type ATPase inhibitor in *P. falciparum*, is also a P-type ATPase inhibitor in *S. cerevisiae*.[10]

Here we report using a synthetic, drug-sensitive *S. cerevisiae* strain that lacks 16 multidrug ABC-transporter export pumps ($ABC_{16}$-Monster strain; GM)[11] to identify the mode of action of an anti-trypanosomal compound. Specifically, we apply directed evolution and whole-genome sequencing to $ABC_{16}$-Monster to identify lanosterol-14-alpha-demethylase (*Sc*CYP51) as the target of MMV001239, a member of the MMV Malaria Box with activity against *T. cruzi*. Our results confirm that resistance-conferring mutations in yeast can be used to predict both the targeted pathway as well as the compound-binding site with a high degree of specificity.

## Results

### Identification of MMV001239, a compound with anti-trypanosomal and anti-yeast activity

As part of an ongoing effort to find antimalarial drug targets, we tested the compounds of the MMV Malaria Box for cytotoxicity against yeast. Since yeast resistance often evolves through mutations in efflux-pump genes rather than true drug targets, we used the $ABC_{16}$-Monster yeast strain[11], a recently engineered strain that entirely lacks sixteen efflux-pump genes and is therefore more sensitive to most cytotoxic compounds. Using a similar approach, we recently identified the *S. cerevisiae* protein PMA1 as the target of the spiroindolone KAE609, a potent antimalarial[10]. The MMV Malaria Box is a set of 400 compounds, including 200 drug-like molecules as well as 200 tool compounds for discovering novel drug-target pathways. This library is freely available to research groups around the world who seek starting points for antimalarial drug discovery. MMV001239, 4-a cyano-N-(5-methoxy-1,3-benzothiazol-2-yl)-N-(pyridin-3-ylmethyl)benzamide, was among the most potent compounds ($IC_{50}$ = 8.1 μM ± 1.2, Fig. 1A), against the drug-sensitive yeast strain, making it an attractive drug candidate for directed-evolution target identification in this system. In contrast, MMV001239 is inactive against wild-type *S. cerevisiae* (i.e., full growth inhibition was not achieved even at 300 μM, the highest concentration tested, Fig. 1A), highlighting the utility of the engineered drug-sensitive strain for target-identification studies.

Given that MMV001239 is a member of the MMV Malaria Box, we first verified its antimalarial activity. Our experiments showed that MMV001239 had weak activity against *P. falciparum* in the asexual stage ($IC_{50}$ = 3.1 μM ± 0.7) compared to other compounds in the MMV box as well as known clinical antimalarials. As a number of the MMV compounds are known to be effective against other eukaryotic parasites including, *T. cruzi*.[12], we tested the compound against *T. cruzi* intracellular amastigotes and confirmed that it is active in this parasite ($IC_{50}$ = 2.01 μM ± 1.10, Fig. 1B).

### MMV001239 targets the sterol biosynthesis pathway in *S. cerevisiae*

To gain insight into the mechanism of action, directed evolution was performed by exposing the $ABC_{16}$-Monster strain to different MMV001239 concentrations in multiple clonal

cultures, as described in the methods. Once strains reached saturation at the highest concentration that permitted growth, single colonies were isolated from drug-containing plates. Four MMV001239-resistant lineages were isolated, and the degree of resistance was determined by comparing their growth in the presence of the inhibitor to that of the non-treated parental strain. Four clonal lineages isolated from these cultures demonstrated 3.2x-, 6.5x-, 2x-, and 5.5x-fold resistance, respectively (Fig. 2A).

To determine the genetic basis of the observed *in vitro* resistance, we isolated genomic DNA from these four lineages for whole-genome sequencing. Samples were sequenced with >40-fold coverage, and the resulting sequences were compared to those of the parental-strain (S288c) reference genome (Table S1). Variants present only in the evolved lines were identified (Table 1). We detected only 4–6 single nucleotide variants (SNV) in each of the four lineages (Table 1). Except for lineage R4, we identified only one nonsynonymous single-nucleotide change per lineage that resulted in an amino-acid change in the encoded protein. No lineage contained insertions or deletions relative to the parental strain. All nonsynonymous mutations in the resistant yeast strains occurred in either *ERG11* or *ERG25*, two genes involved in ergosterol biosynthesis. Lineage R1 and R2 both have nonsynonymous amino-acid changes in the same gene product, *ScERG11*, but in different positions (codons 154 and 318). Lineages R4 and R11 both showed nonsynonymous changes in *ScERG25*, also in different positions (234 and 156). Ergosterol is a sterol component of the plasma membrane in fungi and protozoa that plays a structural role similar to cholesterol in mammalian cells. It is therefore likely that MMV001239 targets this pathway and that these resistant yeast cells were selected because mutations in the associated genes permit growth at high drug concentrations.

Heterozygous deletions in the ergosterol biosynthesis pathway are known to sensitize yeast to a variety of different toxins, presumably because they alter the membrane lipid composition.[13] To further determine whether mutations in *ERG11* or *ERG25* were simply multidrug resistance alleles we examined the complete genome sequences of yeast that had been exposed to 26 additional compounds, mostly from the MMV malaria box until they acquired resistance. Of the 106 sequenced strains, only those exposed to MMV001239 acquired mutations in *ERG11* or *ERG25*. These data demonstrated that these mutations are specific for this compound (Table S2).

The likelihood of finding four independent mutations in the sterol pathway by chance is very low, suggesting that the two gene products identified via directed evolution are both plausible MMV001239 targets. Both genes are essential for the survival of fungi and *T. cruzi*.[14] However, *ScERG25*, which encodes a C-4 methyl sterol oxidase and catalyzes the fifth step in the sterol-biosynthesis pathway, has been replaced by a different set of non-orthologous genes in *T. cruzi*.[15] In addition, the *ScERG25* product is not a known drug target. On the other hand, *ScERG11* encodes lanosterol 14-alpha-demethylase, a cytochrome P450 enzyme that is the target of several antifungals. Furthermore, the *T. cruzi* ortholog of Sc*ERG11* encodes Cyp51p (TcCLB.506297.260), a similarly validated *T. cruzi* drug target.[14, 16, 17] We thus propose that the MMV001239 target is encoded by *ScERG11*. Of note, others have similarly identified pyridine inhibitors of *Sc*ERG11[18], further supporting this hypothesis. To exclude the possibility that observed silent mutations in *FLO1*, *FLO9*, or

other intergenic regions contribute to the resistance phenotype, we used the CRISPR/Cas9 method to engineer the two *ScERG11* mutations found through directed evolution into the parental strain, which was not exposed to MMV001239. Both the original resistant strains and the newly genetically engineered strains have similar MMV001239 $IC_{50}$ values, strengthening our hypothesis that the *ScERG11* mutations cause resistance to MMV001239 (Table 2). The *ScERG25* mutations found in two other resistant lines are likely downstream compensatory mutations that allow yeast cells to grow in the presence of high MMV001239 concentrations. These mutations might be similar in function to the *ERG3* mutations that we and others have found to confer resistance to azoles (*19, 20* and unpublished data). We further tested chemically unrelated compounds in both the CRISPR/Cas9 mutant and parental $ABC_{16}$-Monster strains and found no substantial differences in the $IC_{50}$ values of these compounds, supporting our hypothesis that the mutations in *ScERG11* are specific for MMV001239 rather than contributing to a general resistance mechanism (Table 2).

*Sc*ERG11p catalyzes the C-14 demethylation of lanosterol to form 4,4"-dimethyl cholesta-8,14,24-triene-3-beta-ol. In lineage R1, a valine residue was replaced by glycine (V154G). The conversion of a valine to a glycine is a conservative amino-acid change since both are small, aliphatic amino acids. This amino acid lies near the enzymatic core of the protein, near the center of the heme prosthetic group, in the middle of a highly conserved, active-site-adjacent alpha helix known as the GQHTS alpha-helical region (I-band). Any changes at this site would likely disrupt enzyme functioning and inhibitor-heme binding. In lineage R2, a threonine was replaced by asparagine (T318N). This substitution replaces a polar uncharged residue with one that is slightly bulkier, though still polar and uncharged. This residue is highly conserved across eukaryotic phyla (Fig. 3A). Residue 381 is located on the side of the central enzymatic pocket (Fig. 3B).

*Sc*ERG11p and *Tc*Cyp51p show a high degree of sequence similarity, with 116/383 of the amino acids in the 380-amino-acid aligned region showing identity (p = 1.2 e-50). For the *Sc*ERG11T318N mutation, the homologous *T. cruzi* residue is also a threonine. In contrast, the *Sc*ERG11p valine residue at position 154 is not conserved between *S. cerevisiae* and *T. cruzi*, but the substitution of a glycine for a valine is a conservative amino-acid change. Aside from sequence conservation, functional conservation across the two species has also been reported. *Tc*Cyp51p complements the function of the yeast ERG11 protein when expressed in an *ERG11*-deficient background.[14]

## MMV001239 induces lanosterol and eburicol accumulation in *T. cruzi* membranes, revealing effective Cyp51 inhibition

To further confirm that MMV001239 inhibits *Tc*Cyp51 *in vivo*, we first examined the abundance of sterol-pathway intermediates (Fig. 3C) using gas chromatography/mass spectrometry. As predicted, we found that MMV001239 effectively inhibited the parasite's sterol biosynthesis pathway. Consistent with previous published work, episterol (peak (a) in Fig. 4) and fecosterol (b) are abundant in amastigotes treated with the vehicle (DMSO) or with a compound that targets a different *T. cruzi* pathway (K777, a cruzain inhibitor). Lanosterol (c) and eburicol (e) are synthetic precursors and so remain at low levels if Cyp51 is active. Treatment of infected cultures with both MMV001239 and posaconazole, a known

Cyp51 inhibitor, led to the accumulation of these precursors, detected as high peaks in GC-MS profiles. These findings demonstrate that the sterol biosynthesis pathway was blocked via *T. cruzi* Cyp51 inhibition.

## MMV001239 binds to *T. cruzi* Cyp51

*Sc*ERG11p is the direct target of azole drugs, antifungal small molecules that share a common mechanism of action.[21] Each azole contains a nitrogenous heterocyclic ring that directly binds the central iron atom of the heme prosthetic group. Triazoles such as fluconazole contain five-membered rings with three nitrogens and two carbons. Imidazole antifungals such as ketoconazole contain five-membered rings with only two nitrogens. Although MMV001239 contains a six-membered aromatic ring with a single nitrogen atom, we hypothesize that MMV001239 most likely inhibits *Tc*Cyp51 in a manner similar to the azoles and that the identified amino-acid changes in *Sc*ERG11p confer resistance by interfering with MMV001239 binding.

To investigate whether MMV001239 directly binds to *Tc*Cyp51p, we used a spectrophotometry assay.[22, 23] *Tc*Cyp51p is a cytochrome P450 enzyme with a characteristic spectrophotometric peak at 450 nm when reduced and bound to carbon monoxide. When bound to the endogenous ligand lanosterol (Fig. 3C), spectrophotometry yields a Type 1 spectrum, characterized by a peak and trough around 390 nm and 420 nm, respectively. In contrast, a flipped Type 2 spectrum is seen when an inhibitor such as an azole antifungal is bound, with a trough and peak around 390 nm and 430 nm, respectively, depending on the specific P450 enzyme being studied. We recorded the spectra of *Tc*Cyp51p bound to lanosterol and MMV001239, respectively. As expected, lanosterol binding produced the characteristic Type 1 spectrum. In contrast, MMV001239 exhibits the Type 2 spectrum characteristic of an inhibitor (Supplemental Fig. 1), strengthening our hypothesis that Cyp51 is the direct MMV001239 target in *T. cruzi*.

To evaluate the strength of MMV001239/*Tc*Cyp51 binding, spectral analysis was performed across a range of MMV001239 concentrations. As positive controls, a similar analysis was performed using fluconazole and posaconazole, two well-characterized azoles (Fig. 5A and 5B). The absorbance-peak amplitudes of the various spectra suggest that MMV001239 binding is more similar to that of posaconazole, a potent *Tc*Cyp51p binder, rather than fluconazole, a weak *Tc*Cyp51p binder. However, the binding constants cannot be accurately deduced from these experiments due to the sensitivity limit of the UV-visible-spectroscopy protocol we used, which prohibits measurements at high protein-target concentrations.[24] Thus, we can only conclude that MMV001239 binds *Tc*Cyp51p notably stronger than fluconazole, and weaker than posaconazole.

## Characterizing MMV001239-*Tc*Cyp*51p* binding through X-ray crystallography and molecular docking

As *Tc*Cyp51p is difficult to crystallize in the absence of a strong ligand,[25] we used high-throughput methods to explore possible crystallization conditions. These efforts ultimately yielded *Tc*Cyp51-MMV001239 co-crystals (Supplemental Fig. 2A.). However, despite having a nice appearance, these crystals only diffracted to a resolution of 3.8 Å, allowing us

to visualize only the protein backbone and a fragment of the electron density orthogonal to the heme macrocycle (Supplemental Fig. 2B). The latter suggested that MMV001239 binds via heme-iron coordination, consistent with both 1) the shift of the iron Soret band in the UV-vis binding spectra and 2) the known binding modes of other heme-iron-coordinating nitrogenous heterocycles.

In an independent effort, we used physics-based molecular docking to predict the *Sc*ERG11p/MMV001239 binding pose and compared that predicted pose to structures cocrystallized with lanosterol and fluconazole (Fig. 6). The docked pose occupies the lanosterol catalytic pocket and is similar to the pose of the azole antifungals. The T318N mutation is predicted to sterically hinder inhibitor binding without interfering with the lanosterol-binding site. The V154G mutation may also disrupt the hydrophobic interaction between the cyanide nitrogen and the valine.

To better understand how the *ScERG11* mutations confer MMV001239 resistance, we mapped the evolved amino-acid changes onto *Sc*ERG11p and *Tc*Cyp51p crystal structures. The T318N mutation lies within a highly conserved GQHTS alpha-helical region (I-band) that is similar in both *S. cerevisiae* and *T. cruz*i, both in sequence and structure (Fig. 3a, Fig. 6). T318N maps to a location near the heme-iron-coordinated nitrogenous heterocycle characteristic of all known inhibitors and so may sterically hinder inhibitor binding without affecting the lanosterol binding site (Fig. 6). The V154G mutation lies adjacent to the inner pocket, but in a structurally conserved region that does not interact with any known azoles. It is possible that the change to a glycine changes protein dynamics due to increased flexibility of the polypeptide chain as observed in a previous study.[26] However, the homologous amino acid in *T. cruzi* does lie adjacent to the crystallographic binding poses of many preclinical anti-trypanosomal Cyp51 inhibitors (Fig. 6). We therefore hypothesize that the mechanism of MMV001239 resistance due to both mutations in *ERG11* can be best explained if MMV001239 has a binding pose similar to that of other azoles.

## Discussion

Target identification is a major barrier to subsequent drug development that inevitably follows hit identification via phenotypic screening. One path to target identification is the use of *in vitro* directed evolution and subsequent whole-genome sequencing (WGS).[27–32] However, the advantages and limitations of directed evolution are organism dependent. Many organisms are difficult to culture, have lengthy cell cycles, possess large diploid genomes, and/or express multidrug efflux pumps that complicate resistance selection by conferring generic drug insensitivity.[33]

Although target identification through directed evolution can be performed in *T. cruzi*, it is very time consuming. A recent effort that identified cytochrome b as a target of the experimental small-molecule inhibitor GNF7686 took eleven months, ultimately producing a single lineage with a mere 4-fold $IC_{50}$ shift.[34] In that study, multiple independent lineages were not possible because maintaining *T. cruzi* cultures is labor intensive. If the identified mutation had not been in a gene that had already been extensively studied as a drug target in multiple species, interpretation of this result might have been difficult. Furthermore,

cytochrome b is encoded by the *T. cruzi* haploid mitochondrial genome, possibly facilitating the emergence of resistance clones as well as the detection of the mutation. As in the case described here, *Saccharomyces* was used to support the hypothesis that cytochrome b was indeed the GNF7686 target; several strains with haploinsufficient mutations in respiration genes showed GNF7686 sensitivity.

In contrast to this study of the eukaryotic pathogen, directed evolution in drug-sensitive yeast identified the MMV001239 target quickly and effectively. Selection in yeast required only 3–9 days, easily permitting four selections. The only resistance-conferring mutations in these four lineages occurred in two genes that both encode proteins of the ergosterol biosynthesis pathway. Furthermore, half of the mutations were in the binding site of the drug's molecular target. The high specificity of this approach is especially striking when compared with high-throughput approaches such as haploinsufficiency profiling,[35, 36] chemical pull-downs,[37] overexpression studies,[38] and other biochemical assays, which often implicate many genes rather than just the single target.[33] In addition, since drug selection theoretically queries all possible mutations, unlike haploinsufficiency profiling or biochemical pull-downs, it is able to provide a more specific answer while searching a much larger data set. However, each of these methods has its own strengths and weaknesses and can be used complementarily to identify and characterize the targets of chemical compounds and the genes involved in the target pathway and drug resistance.

In these experiments we found no mutations in genes associated with pleiotropic drug resistance (e.g., the transcription factor, *YRR1*), although these types of mutations have emerged in experiments with other compounds such as the spiroindolone KAE609.[39] As more resistance profiles are collected, more genes that contribute to the generic resistome will be identified, enabling better discrimination between real signal and background noise. The use of the $ABC_{16}$-Monster *S. cerevisiae* strain, which lacks sixteen export pumps, also reduces the likelihood of evolved resistance via mutations in general resistance genes.

On the other hand, our method is not without its limitations. It requires that the target class, if not the actual target, be conserved between *Saccharomyces* and the species of interest. In addition, we have found that only about a third of compounds that are active against eukaryotic pathogens inhibit yeast growth in a reasonable range. For compounds that have activity that is specific to trypanosomes such as *T. brucei*, genome-wide RNA interference studies could be more useful.[40–44]

Finally, that Cyp51 is a known *T. cruzi* target was certainly helpful in the current study. It is well known that ergosterol is essential for cell-membrane integrity in *T. cruzi*, an organism that is unable to utilize host cholesterol.[45] Furthermore, the genes for ergosterol biosynthesis are expressed in all phases of the *T. cruzi* life cycle, and Cyp51 plays an essential role in that pathway.[46] Inhibitors of sterol 14α-demethylase (Cyp51) have also proven effective against *T. cruzi in vitro* and *in vivo*, making the enzyme a viable target for the treatment of Chagas disease.[47, 48] Recently, high-throughput target-based screens using recombinant *Tc*Cyp51 have led to the development of several next-generation anti-trypanosomal small molecules. Like MMV001239, some of these contain pyridine groups that have been shown through co-crystallography to bind to the central *Tc*Cyp51 heme molecule.[49]

It is still not clear that Cyp51 inhibitors can eliminate human disease. Recently, clinical studies evaluated whether the antifungal drugs posaconazole and ravuconazole[50, 51] could be repurposed for the treatment of Chagas disease. These Cyp51 inhibitors are effective against the parasite *in vitro* and in some animal models.[52] Disappointingly, they both showed only low efficacy in the treatment of Chagas disease in humans.[53] Since both posaconazole and ravuconazole were originally developed as antifungal drugs and therefore were not necessarily optimized for the *T. cruzi* 14-demethylase enzyme, future structure-based approaches could be used to identify and optimize more effective *T. cruzi* Cyp51 inhibitors.[17] MMV001239 can now be added to this growing list of antitrypanosomal Cyp51 inhibitors. While its binding pose is similar to other investigational compounds, its unique structure may now be further optimized to improve potency and/or reduce toxicity,.

## Methods

### Chemical Information

The IUPAC name of MMV001239 is 4-cyano-N-(5-methoxy-1,3-benzothiazol-2-yl)-N-(pyridin-3-ylmethyl)benzamide. The chemical was purchased from Life Chemicals Inc. (catalog #F2515-1937) through MolPort. The purity of the compound was evaluated by mass spectrometry and determined to be 89.4% pure.

### *S. cerevisiae* susceptibility and dose-response assay

$ABC_{16}$-Monster yeast cells were inoculated from agar plates into 2 ml of liquid YPD media and grown to saturation (OD600 > 1.0) overnight at 250 RPM in a shaking incubator at 30°C. Cultures were diluted to OD600 0.01 in 3.5 ml of YPD and grown to log phase. 100 µl of cells were added to the wells of a 96-well plate. Compounds were added starting with a concentration of 150 µM, followed by 1:2 serial dilutions. An initial reading of OD600 (t = 0 hrs) was taken using a Synergy HT spectrophotometer, and cells were incubated for a period of 18 hours at 30°C. After incubation, plates were shaken for 30 seconds on the “high” setting and read at OD600. Cells grown in the absence of drugs were used as a negative control. Percent growth was calculated using the formula $Ab600_{treated}/Ab600_{control} \times 100$

$IC_{50}$ values were determined by first subtracting the OD600 values at t=0 from those of the final reading and then utilizing Graphpad Prism to calculate nonlinear regression on log(inhibitor) vs. response with variable slope (four parameters).

### $IC_{50}$ Determination for *P. falciparum*

Drug susceptibility was measured using the 72-hour malaria SYBR® Green I-based fluorescence assay, as previously reported.[54] Each compound was tested in technical duplicate via ten-point concentration curve prepared by three-fold dilution starting at 6.7 µM. Three independent experiments were carried out for MMV001239 and $IC_{50}$ values were calculated using nonlinear regression curve fit in GraphPad Prism 6.0.

### Selection of MMV001239-resistant *S. cerevisiae*

Strains are listed in Table S4. Assorted concentrations of the inhibitor were added to 50 ml conical tubes containing 20 µl of saturated $ABC_{16}$-Monster cells in 20 ml of YPD. Each

selection was cultured under vigorous shaking until the culture reached saturation. Saturated cultures were diluted into fresh media with the inhibitors, and multiple rounds of selection were performed at increasingly higher concentrations. After reaching a compound concentration that was substantially higher than that of the initial $IC_{50}$ concentration, polyclonal cultures were streaked onto agar plates containing the appropriate inhibitor concentration. Single colonies were isolated, and $IC_{50}$ assays were performed to determine the degree of evolved resistance vs. that of the parental strain.

### Statistical tests used for $IC_{50}$ analysis

P values for $IC_{50}$ fold changes were determined using a one-tailed ratio paired t-test, which compared the ratio of the mutant-strain $IC_{50}$ value to that of the parental strain.

### Whole-genome sequencing and analysis

DNA was extracted from yeast cells using the YeaStar Genomic DNA kit. For whole-genome sequencing (WGS), genomic yeast DNA libraries were normalized to 0.2 ng/μL and prepared for sequencing according to the manufacturer's instructions using the Illumina Nextera XT kit whole-genome resequencing library (see the Illumina protocol of tagmentation followed by ligation, v. 2013, Illumina, Inc., San Diego). DNA libraries were clustered and run on an Illumina HiSeq as 2×100 paired end reads, according to the manufacturer's instructions. Base calls were made using the software CASAVA v1.8.2. Initial sequence alignments were performed using the platypus software.[55] Reads were aligned to the reference *S. cerevisiae* genome using BWA, and unmapped reads were filtered using SAMTools. SNPs were called using GATK and filtered using the platypus software.

### CRISPR-Cas9 Genome Engineering in *S. cerevisiae* via Homology Directed Repair

CRISPR/Cas9 allelic exchange was performed using the *S. cerevisiae* $ABC_{16}$-Monster strain and the p414 and p426 vectors from the Church lab (Addgene) as previously described[56], with the exception that the *trp* selection marker of p414 was replaced with *met15* for compatibility with the $ABC_{16}$-Monster strain. Briefly, Cas9 expressing $ABC_{16}$-Monster yeast cells were obtained via standard lithium acetate transformation[57] of *met15*-modified p414 plasmid and grown on CM-glucose plates lacking methionine.

In order to generate the *cyp51*-specific gRNA plasmid based on vector p426, oligonucleotides matching the target sequence were synthesized (Integrated DNA Technologies) with a 24 base-pair overlap with the gRNA expression vector backbone in both the forward and reverse directions (p426)[56]. The new vector with *cyp51* gRNAs (Table S5) was generated via PCR, transformed into *E. coli* XL-10 gold competent cells (Agilent), and selected on plates containing LB-Ampicillin[58]. DNA from these colonies was purified (QiaQuick Miniprep Kit, Qiagen) and the presence of the new gRNAs confirmed via Sanger sequencing.

$ABC_{16}$-Monster yeast cells constitutively expressing Cas9 were transformed with 250–500 ng of gRNA expression vector via a standard lithium acetate transformation method using 1 nmole donor template[57]. To select for $ABC_{16}$-Monster yeast containing the transformed DNA, cells were grown on CM glucose agar plates lacking methionine and leucine.

Sanger sequencing was performed to verify each mutation (Eton Bioscience). Cells were cultured in YPD complete media to induce the loss of the Cas9 and gRNA plasmids.

### Cyp51 binding-affinity assay by UV-visible spectroscopy

0.5 μl of compounds at different concentrations (0.1 to 100 μM in DMSO) were assayed in 100 mM potassium phosphate buffer (pH 7.5) containing 10% glycerol in the absence or presence of 2.4 μM Cyp51.[59] Ligand binding was measured in 96-well plates, in duplicate. Absorption spectra were recorded from 350 nm to 500 nm in 10 nm increments using a Synergy HT spectrophotometer. To correct for the organic-solvent effect, the same volume of DMSO was added to a reference well. Binding affinities were approximated from the titration curves by calculating the absorption shift (ΔA) between 420 and 390 nm for the indicated ligand concentrations, using the algorithm described in reference.[24]

### GC-MS analysis of *T. cruzi* sterols

Sterol characterization of *T. cruzi* intracellular amastigotes was performed as previously described, with minor modifications.[24] Briefly, mouse myoblasts (C2C12, ATCC #CRL-1772) were infected with the *T. cruzi* CAI/72 strain, in a multiplicity of infection of 1:20. After 72h of infection, cultures were treated with sub-cidal compound doses for 24h to induce the inhibition of sterol biosynthesis without completely killing the parasites. Posaconazole (100 nM) was used as a positive control, and Benznidazole (5 μM), which targets different pathways, was used as a negative control. MMV001239 was tested at 3 μM.

For the extractions, the infected cultures were detached and pelleted, and the lipids were extracted with chloroform/methanol, chloroform, and acetonitrile. Following each step, polar molecules were eliminated via triple washes with water and the organic layer was dried under $N_2$ flow to allow solvent exchange. The sterols were then submitted to chemical derivatization of trimethylsilyl (TMS) groups with 70 μL of N,N-bis(trimethylsilyl)-2,2,2-trifluoroacetamide (BSTFA) and 70 μL of hexane for 2h at 37°C. Three μL of the TMS-derivatized lipid mixture was injected directly into an Agilent 7820A gas-chromatography system coupled to a mass-selective detector. The lipids were separated on the analytical column using a temperature profile that begins at 200°C for 3 min, increases by 15°C/min to 270 °C, and then holds at 270°C for 30 min, finishing with post run 280°C, 4 min. The mass spectrometer scanned from m/z 50 to 750 over the course of analysis.

### Compound-activity assessment against intracellular *T. cruzi* amastigote

The mouse myoblast cell line C2C12 (ATCC #CRL-1772) was maintained at 37°C with 5% $CO_2$ in Dulbecco's Modified Eagle's Medium (DMEM) containing 4.5 g/l glucose, supplemented with 5% fetal bovine serum (FBS), 100 U/ml penicillin, and 100 μg/ml streptomycin. *T. cruzi* CA-I/72 culture-derived trypomastigotes were obtained from infected C2C12 culture supernatants after six days of infection. Cells and parasites were seeded in 384-well black clear-bottom plates at $1.5 \times 10^5$ parasites/mL and $1.0 \times 10^4$ C2C12/mL density in 50 μl of DMEM media per well. Compounds were added immediately after infection, and plates were incubated for 72 hours at 37°C 5% $CO_2$. Plates were fixed with 4% formaldehyde for at least one hour and stained with 0.5 μg/ml of 4',6-diamidino-2-phenylindole (DAPI) for four hours. Plates were then washed twice and imaged using

ImageXpress Micro XL (Molecular Devices). Images were analyzed by dedicated algorithms developed using the MetaXpress software. Antiparasitic activity was normalized based on negative controls (vehicle wells) and positive controls (uninfected wells). Host-cell viability was determined based on the total number of C2C12 cells in each well relative to the average number of host cells in vehicle wells.

## Crystallography

To determine the MMV001239 binding mode, recombinant *Tc*Cyp51, modified by replacing the first 31 residues upstream of Pro32 with the fragment MAKKTSSKGKL[60] and by inserting a $His_6$-tag at the C-terminus, was expressed and purified as described elsewhere.[61] Concentrated, purified protein samples were stored at −80 °C and diluted to 0.1 mM prior to crystallization by mixing with 20 mM potassium phosphate (pH 7.5), 10% glycerol, 1 mM DTT, and 0.5 mM EDTA, supplemented with equimolar inhibitor.

Crystallization conditions were determined using commercial high-throughput screening kits available in deep-well format (Hampton Research, Aliso Viejo, CA), a nanoliter drop-setting Mosquito robot (TTP LabTech, Cambridge, MA) operating with 96-well plates, and a hanging drop crystallization protocol. Crystals were further optimized in 24-well plates for diffraction data collection and harvested from the 2-μL drops containing 0.1 M HEPES, pH 7.5, 4% isopropanol, 6% PEG 3350, and 7.8 mM detergent (n-Nonyl-beta-D-maltoside). Prior to data collection, crystals were cryo-protected by first plunging them into a drop of reservoir solution supplemented with 20% ethylene glycol, and then flash freezing them in liquid nitrogen.

Diffraction data were collected at 100–110 K at beamline 8.3.1, Advanced Light Source, Lawrence Berkeley National Laboratory, USA. Data indexing, integration, and scaling were conducted using MOSFLM[62] and the programs implemented in the ELVES software suite.[63] The crystal structures were determined by molecular replacement using diffraction data processed in the $P3_121$ space groups, with the atomic coordinates of *T. cruzi* Cyp51 (PDB ID code: 4C0C) serving as a search model. Model refinement was performed using the REFMAC5 software.[64, 65] Data collection and refinement statistics are shown in Table S3.

## Small-Molecule Docking

A crystal structure of *S. cerevisiae* lanosterol 14-alpha demethylase (PDB ID: 4K0F[66]) was obtained from the Protein Data Bank.[67] This structure was processed with Schrödinger's Protein Preparation Wizard, which added hydrogen atoms at pH 7.0 using PROPKA,[68] converted selenomethionine residues to methionine residues, and optimized the protein geometry using the OPLS_2005 force field[69, 70] until the heavy-atom RMSD converged to 0.30 Å. Models of two known ligands (itraconazole and MMV001239) were prepared using Schrödinger's LigPrep module. Ligand geometries were optimized using the OPLS_2005 force field. All protonation states appropriate for pH 7.0 +/− 2.0 were similarly considered.

The known ligands were docked into the target structure using Schrödinger's Glide XP (default parameters).[71–74] A docking constraint was employed to encourage coordination with the heme metal atom where appropriate. Glide XP recaptured the crystallographic pose of itraconazole, included in the docking study as a positive control. The orientation of the

MMV001239 nitrogenous heterocycle was manually adjusted only slightly to improve coordination with the heme iron atom.

## Supplementary Material

Refer to Web version on PubMed Central for supplementary material.

## Acknowledgments

S.O. and G.M.G. are supported by the Bill and Melinda Gates Foundation, Grand Challenge in Global Health Exploration Grant (OPP1086217, OPP1141300). G.M.G. is also supported by the UC San Diego Medical Scientist Training Program (T32 GM007198-40) and the DoD National Defense Science and Engineering Fellowship Program. E.A.W. is supported by grants from the NIH (5R01AI090141 and R01AI103058). Y.S. was partially supported by the NIH (UL1TR000100). Support from the National Biomedical Computation Resource (NBCR, NIH P41 GM103426) and the New Innovator Award (NIH DP2 OD007237) to R.E.A. is also gratefully acknowledged. L.I.M. is supported by the Canadian Institutes of Health Research (#338511). L.M.P. is supported by the NIH (AI095437). Whole-genome sequencing was conducted at the IGM Genomics Center, University of California, San Diego, La Jolla, CA (P30DK063491, P30CA023100). The Advanced Light Source is supported by the Director, Office of Science, Office of Basic Energy Sciences, of the U.S. Department of Energy under Contract No. DE-AC02-05CH11231. Mass spectrometry was performed by UCSD Chemistry and Biochemistry Mass Spectrometry Facility. We would like to acknowledge Omar Vandal of the Bill and Melinda Gates Foundation for help and advice.

## References

1. Lee BY, Bacon KM, Bottazzi ME, Hotez PJ. Global economic burden of Chagas disease: a computational simulation model. Lancet Infect Dis. 2013; 13:342–348. [PubMed: 23395248]
2. Rassi A, Rassi A, Marin-Neto JA. Chagas disease. Lancet. 2010; 375:1388–1402. [PubMed: 20399979]
3. Castro JA, de Mecca MM, Bartel LC. Toxic side effects of drugs used to treat Chagas' disease (American trypanosomiasis). Hum Exp Toxicol. 2006; 25:471–479. [PubMed: 16937919]
4. Institute, P. H. R. BENEFIT trial: Evaluation of the use of antiparasital drug (benznidazole) in the treatment of chronic Chagas' disease. 2004 (Identifier: NCT00123916).
5. Morillo CA, Marin-Neto JA, Avezum A, Sosa-Estani S, Rassi A Jr, Rosas F, Villena E, Quiroz R, Bonilla R, Britto C, Guhl F, Velazquez E, Bonilla L, Meeks B, Rao-Melacini P, Pogue J, Mattos A, Lazdins J, Rassi A, Connolly SJ, Yusuf S, Investigators, B. Randomized Trial of Benznidazole for Chronic Chagas' Cardiomyopathy. N Engl J Med. 2015; 373:1295–1306. [PubMed: 26323937]
6. Marin-Neto JA, Rassi A, Avezum A, Mattos AC, Rassi A. The BENEFIT trial: testing the hypothesis that trypanocidal therapy is beneficial for patients with chronic Chagas heart disease. Mem I Oswaldo Cruz. 2009; 104:319–324.
7. Altcheh J, Moscatelli G, Moroni S, Garcia-Bournissen F, Freilij H. Adverse Events After the Use of Benznidazole in Infants and Children With Chagas Disease. Pediatrics. 2011; 127:E212–E218. [PubMed: 21173000]
8. Sykes ML, Baell JB, Kaiser M, Chatelain E, Moawad SR, Ganame D, Ioset JR, Avery VM. Identification of Compounds with Anti-Proliferative Activity against Trypanosoma brucei brucei Strain 427 by a Whole Cell Viability Based HTS Campaign. Plos Neglect Trop D. 2012; 6
9. Hoepfner D, McNamara CW, Lim CS, Studer C, Riedl R, Aust T, McCormack SL, Plouffe DM, Meister S, Schuierer S, Plikat U, Hartmann N, Staedtler F, Cotesta S, Schmitt EK, Petersen F, Supek F, Glynne RJ, Tallarico JA, Porter JA, Fishman MC, Bodenreider C, Diagana TT, Movva NR, Winzeler EA. Selective and Specific Inhibition of the Plasmodium falciparum Lysyl-tRNA Synthetase by the Fungal Secondary Metabolite Cladosporin. Cell Host Microbe. 2012; 11:654–663. [PubMed: 22704625]
10. Goldgof GM, Durrant JD, Ottilie S, Vigil E, Allen KE, Gunawan F, Kostylev M, Henderson KA, Yang J, Schenken J, LaMonte GM, Manary MJ, Murao A, Nachon M, Stanhope R, Prescott M, McNamara CW, Slayman CW, Amaro RE, Suzuki Y, Winzeler EA. Comparative chemical

genomics reveal that the spiroindolone antimalarial KAE609 (Cipargamin) is a P-type ATPase inhibitor. Sci Rep. 2016; 6:27806. [PubMed: 27291296]

11. Suzuki Y, St Onge RP, Mani R, King OD, Heilbut A, Labunskyy VM, Chen W, Pham L, Zhang LV, Tong AH, Nislow C, Giaever G, Gladyshev VN, Vidal M, Schow P, Lehar J, Roth FP. Knocking out multigene redundancies via cycles of sexual assortment and fluorescence selection. Nat Methods. 2011; 8:159–164. [PubMed: 21217751]
12. Kaiser M, Maes L, Tadoori LP, Spangenberg T, Ioset JR. Repurposing of the Open Access Malaria Box for Kinetoplastid Diseases Identifies Novel Active Scaffolds against Trypanosomatids. J Biomol Screen. 2015; 20:634–645. [PubMed: 25690568]
13. Hoepfner D, Helliwell SB, Sadlish H, Schuierer S, Filipuzzi I, Brachat S, Bhullar B, Plikat U, Abraham Y, Altorfer M, Aust T, Baeriswyl L, Cerino R, Chang L, Estoppey D, Eichenberger J, Frederiksen M, Hartmann N, Hohendahl A, Knapp B, Krastel P, Melin N, Nigsch F, Oakeley EJ, Petitjean V, Petersen F, Riedl R, Schmitt EK, Staedtler F, Studer C, Tallarico JA, Wetzel S, Fishman MC, Porter JA, Movva NR. High-resolution chemical dissection of a model eukaryote reveals targets, pathways and gene functions. Microbiological research. 2014; 169:107–120. [PubMed: 24360837]
14. Buckner FS, Joubert BM, Boyle SM, Eastman RT, Verlinde CL, Matsuda SP. Cloning and analysis of Trypanosoma cruzi lanosterol 14alpha-demethylase. Mol Biochem Parasitol. 2003; 132:75–81. [PubMed: 14599667]
15. Cosentino RO, Aguero F. Genetic profiling of the isoprenoid and sterol biosynthesis pathway genes of Trypanosoma cruzi. PLoS One. 2014; 9:e96762. [PubMed: 24828104]
16. Lepesheva GI, Villalta F, Waterman MR. Targeting Trypanosoma cruzi sterol 14alpha-demethylase (CYP51). Adv Parasitol. 2011; 75:65–87. [PubMed: 21820552]
17. Buckner FS, Urbina JA. Recent Developments in Sterol 14-demethylase Inhibitors for Chagas Disease. Int. J. Parasitol. Drugs Drug Resist. 2012; 2:236–242. [PubMed: 23277882]
18. Hoepfner D, Karkare S, Helliwell SB, Pfeifer M, Trunzer M, De Bonnechose S, Zimmerlin A, Tao J, Richie D, Hofmann A, Reinker S, Frederiksen M, Movva NR, Porter JA, Ryder NS, Parker CN. An integrated approach for identification and target validation of antifungal compounds active against Erg11p. Antimicrob. Agents Chemother. 2012; 56:4233–4240. [PubMed: 22615293]
19. Morio F, Pagniez F, Lacroix C, Miegeville M, Le Pape P. Amino acid substitutions in the Candida albicans sterol Delta5,6-desaturase (Erg3p) confer azole resistance: characterization of two novel mutants with impaired virulence. J Antimicrob Chemother. 2012; 67:2131–2138. [PubMed: 22678731]
20. Martel CM, Parker JE, Bader O, Weig M, Gross U, Warrilow AG, Rolley N, Kelly DE, Kelly SL. Identification and characterization of four azole-resistant erg3 mutants of Candida albicans. Antimicrob Agents Chemother. 2010; 54:4527–4533. [PubMed: 20733039]
21. Kalb VF, Woods CW, Turi TG, Dey CR, Sutter TR, Loper JC. Primary structure of the P450 lanosterol demethylase gene from Saccharomyces cerevisiae. DNA. 1987; 6:529–537. [PubMed: 3322742]
22. von Kries JP, Warrier T, Podust LM. Identification of small-molecule scaffolds for p450 inhibitors. Curr Protoc Microbiol. 2010 Chapter 17, Unit17 14.
23. Podust LM, von Kries JP, Eddine AN, Kim Y, Yermalitskaya LV, Kuehne R, Ouellet H, Warrier T, Altekoster M, Lee JS, Rademann J, Oschkinat H, Kaufmann SH, Waterman MR. Small-molecule scaffolds for CYP51 inhibitors identified by high-throughput screening and defined by X-ray crystallography. Antimicrob. Agents Chemother. 2007; 51:3915–3923. [PubMed: 17846131]
24. Gunatilleke SS, Calvet CM, Johnston JB, Chen CK, Erenburg G, Gut J, Engel JC, Ang KK, Mulvaney J, Chen S, Arkin MR, McKerrow JH, Podust LM. Diverse inhibitor chemotypes targeting Trypanosoma cruzi CYP51. PLoS Negl Trop Dis. 2012; 6:e1736. [PubMed: 22860142]
25. Choi JY, Podust LM, Roush WR. Drug Strategies Targeting CYP51 in Neglected Tropical Diseases. Chem Rev. 2014; 114:11242–11271. [PubMed: 25337991]
26. Podust LM, Poulos TL, Waterman MR. Crystal structure of cytochrome P450 14alpha -sterol demethylase (CYP51) from Mycobacterium tuberculosis in complex with azole inhibitors. Proc Natl Acad Sci U S A. 2001; 98:3068–3073. [PubMed: 11248033]

27. Jones DC, Foth BJ, Urbaniak MD, Patterson S, Ong HB, Berriman M, Fairlamb AH. Genomic and Proteomic Studies on the Mode of Action of Oxaboroles against the African Trypanosome. PLoS Negl Trop Dis. 2015; 9:e0004299. [PubMed: 26684831]
28. Li J, Yuan J, Cheng KC, Inglese J, Su XZ. Chemical genomics for studying parasite gene function and interaction. Trends Parasitol. 2013; 29:603–611. [PubMed: 24215777]
29. Herman JD, Pepper LR, Cortese JF, Estiu G, Galinsky K, Zuzarte-Luis V, Derbyshire ER, Ribacke U, Lukens AK, Santos SA, Patel V, Clish CB, Sullivan WJ Jr, Zhou H, Bopp SE, Schimmel P, Lindquist S, Clardy J, Mota MM, Keller TL, Whitman M, Wiest O, Wirth DF, Mazitschek R. The cytoplasmic prolyl-tRNA synthetase of the malaria parasite is a dual-stage target of febrifugine and its analogs. Sci Transl Med. 2015; 7:288ra277.
30. Vaidya AB, Morrisey JM, Zhang ZS, Das S, Daly TM, Otto TD, Spillman NJ, Wyvratt M, Siegl P, Marfurt J, Wirjanata G, Sebayang BF, Price RN, Chatterjee A, Nagle A, Stasiak M, Charman SA, Angulo-Barturen I, Ferrer S, Jimenez-Diaz MB, Martinez MS, Gamo FJ, Avery VM, Ruecker A, Delves M, Kirk K, Berriman M, Kortagere S, Burrows J, Fan E, Bergman LW. Pyrazoleamide compounds are potent antimalarials that target Na+ homeostasis in intraerythrocytic Plasmodium falciparum. Nat. Commun. 2014; 5
31. Sergeev G, Roy S, Jarek M, Zapolskii V, Kaufmann DE, Nandy RK, Tegge W. High-throughput screening and whole genome sequencing identifies an antimicrobially active inhibitor of Vibrio cholerae. BMC Microbiol. 2014; 14:49. [PubMed: 24568688]
32. Ioerger TR, O'Malley T, Liao R, Guinn KM, Hickey MJ, Mohaideen N, Murphy KC, Boshoff HI, Mizrahi V, Rubin EJ, Sassetti CM, Barry CE 3rd, Sherman DR, Parish T, Sacchettini JC. Identification of new drug targets and resistance mechanisms in Mycobacterium tuberculosis. PLoS One. 2013; 8:e75245. [PubMed: 24086479]
33. Zheng XS, Chan TF, Zhou HH. Genetic and genomic approaches to identify and study the targets of bioactive small molecules. Chem. Biol. 2004; 11:609–618. [PubMed: 15157872]
34. Khare S, Roach SL, Barnes SW, Hoepfner D, Walker JR, Chatterjee AK, Neitz RJ, Arkin MR, McNamara CW, Ballard J, Lai Y, Fu Y, Molteni V, Yeh V, McKerrow JH, Glynne RJ, Supek F. Utilizing Chemical Genomics to Identify Cytochrome b as a Novel Drug Target for Chagas Disease. PLoS Pathog. 2015; 11:e1005058. [PubMed: 26186534]
35. Giaever G, Chu AM, Ni L, Connelly C, Riles L, Veronneau S, Dow S, Lucau-Danila A, Anderson K, Andre B, Arkin AP, Astromoff A, El-Bakkoury M, Bangham R, Benito R, Brachat S, Campanaro S, Curtiss M, Davis K, Deutschbauer A, Entian KD, Flaherty P, Foury F, Garfinkel DJ, Gerstein M, Gotte D, Guldener U, Hegemann JH, Hempel S, Herman Z, Jaramillo DF, Kelly DE, Kelly SL, Kotter P, LaBonte D, Lamb DC, Lan N, Liang H, Liao H, Liu L, Luo C, Lussier M, Mao R, Menard P, Ooi SL, Revuelta JL, Roberts CJ, Rose M, Ross-Macdonald P, Scherens B, Schimmack G, Shafer B, Shoemaker DD, Sookhai-Mahadeo S, Storms RK, Strathern JN, Valle G, Voet M, Volckaert G, Wang CY, Ward TR, Wilhelmy J, Winzeler EA, Yang Y, Yen G, Youngman E, Yu K, Bussey H, Boeke JD, Snyder M, Philippsen P, Davis RW, Johnston M. Functional profiling of the Saccharomyces cerevisiae genome. Nature. 2002; 418:387–391. [PubMed: 12140549]
36. Winzeler EA, Shoemaker DD, Astromoff A, Liang H, Anderson K, Andre B, Bangham R, Benito R, Boeke JD, Bussey H, Chu AM, Connelly C, Davis K, Dietrich F, Dow SW, El Bakkoury M, Foury F, Friend SH, Gentalen E, Giaever G, Hegemann JH, Jones T, Laub M, Liao H, Liebundguth N, Lockhart DJ, Lucau-Danila A, Lussier M, M'Rabet N, Menard P, Mittmann M, Pai C, Rebischung C, Revuelta JL, Riles L, Roberts CJ, Ross-MacDonald P, Scherens B, Snyder M, Sookhai-Mahadeo S, Storms RK, Veronneau S, Voet M, Volckaert G, Ward TR, Wysocki R, Yen GS, Yu K, Zimmermann K, Philippsen P, Johnston M, Davis RW. Functional characterization of the S. cerevisiae genome by gene deletion and parallel analysis. Science. 1999; 285:901–906. [PubMed: 10436161]
37. Drewes G, Faulstich H. The enhanced ATPase activity of glutathione-substituted actin provides a quantitative approach to filament stabilization. J Biol Chem. 1990; 265:3017–3021. [PubMed: 2137454]
38. Begolo D, Erben E, Clayton C. Drug target identification using a trypanosome overexpression library. Antimicrob. Agents Chemother. 2014; 58:6260–6264. [PubMed: 25049244]

39. Goldgof GM, Durrant JD, Ottilie S, Vigil E, Allen KE, Gunawan F, Kostylev M, Henderson KA, Yang J, Schenken J, LaMonte GM, Manary MJ, Murao A, Nachon M, Stanhope R, Prescott M, McNamara CW, Slayman CW, Amaro RE, Suzuki Y, Winzeler EA. Comparative chemical genomics reveal that the spiroindolone antimalarial KAE609 (Cipargamin) is a P-type ATPase inhibitor. Scientific Reports. 2016 *In press*.
40. Baker N, Alsford S, Horn D. Genome-wide RNAi screens in African trypanosomes identify the nifurtimox activator NTR and the eflornithine transporter AAT6. Mol Biochem Parasitol. 2011; 176:55–57. [PubMed: 21093499]
41. Alsford S, Eckert S, Baker N, Glover L, Sanchez-Flores A, Leung KF, Turner DJ, Field MC, Berriman M, Horn D. High-throughput decoding of antitrypanosomal drug efficacy and resistance. Nature. 2012; 482:232–236. [PubMed: 22278056]
42. Zoltner M, Leung KF, Alsford S, Horn D, Field MC. Modulation of the Surface Proteome through Multiple Ubiquitylation Pathways in African Trypanosomes. PLoS Pathog. 2015; 11:e1005236. [PubMed: 26492041]
43. Alsford S, Turner DJ, Obado SO, Sanchez-Flores A, Glover L, Berriman M, Hertz-Fowler C, Horn D. High-throughput phenotyping using parallel sequencing of RNA interference targets in the African trypanosome. Genome Res. 2011; 21:915–924. [PubMed: 21363968]
44. Horn D. High-throughput decoding of drug targets and drug resistance mechanisms in African trypanosomes. Parasitology. 2014; 141:77–82. [PubMed: 23561654]
45. Liendo A, Visbal G, Piras MM, Piras R, Urbina JA. Sterol composition and biosynthesis in Trypanosoma cruzi amastigotes. Mol Biochem Parasitol. 1999; 104:81–91. [PubMed: 10589983]
46. de Macedo-Silva ST, de Souza W, Rodrigues JC. Sterol Biosynthesis Pathway as an Alternative for the Anti-Protozoan Parasite Chemotherapy. Curr Med Chem. 2015; 22:2186–2198. [PubMed: 25787966]
47. Flynn K, Lang AP. Sudden nocturnal death in refugee from Vietnam. CMAJ. 1988; 139:374.
48. Urbina JA. Ergosterol biosynthesis and drug development for Chagas disease. Mem Inst Oswaldo Cruz. 2009; 104(Suppl 1):311–318. [PubMed: 19753490]
49. Calvet CM, Vieira DF, Choi JY, Kellar D, Cameron MD, Siqueira-Neto JL, Gut J, Johnston JB, Lin L, Khan S, McKerrow JH, Roush WR, Podust LM. 4-Aminopyridyl-based CYP51 inhibitors as anti-Trypanosoma cruzi drug leads with improved pharmacokinetic profile and in vivo potency. J Med Chem. 2014; 57:6989–7005. [PubMed: 25101801]
50. Torrico, F. E1224/benznidazole trial (DNDi-Eisai, Bolivia): E1224-Results of proof of concept clinical trial in patients with chronic indeterminate Chagas disease. 62nd Annual Meeting of the American Society of Tropical Medicine and Hygiene; Washington, DC. 2013.
51. Diseases, D. f. N. Proof-of-concept study of E1224 to treat adult patients with Chagas Disease. 2011 (Identifier: NCT01489228. Sponsor: Drugs for Neglected Diseases).
52. Khare S, Liu X, Stinson M, Rivera I, Groessl T, Tuntland T, Yeh V, Wen B, Molteni V, Glynne R, Supek F. Antitrypanosomal Treatment with Benznidazole Is Superior to Posaconazole Regimens in Mouse Models of Chagas Disease. Antimicrob. Agents Chemother. 2015; 59:6385–6394. [PubMed: 26239982]
53. Diseases, D. f. N.. Drug trial for leading parasitic killer of the Americas shows mixed results but provides new evidence for improved therapy. Washington, DC: 2013.
54. Johnson JD, Dennull RA, Gerena L, Lopez-Sanchez M, Roncal NE, Waters NC. Assessment and continued validation of the malaria SYBR green I-based fluorescence assay for use in malaria drug screening. Antimicrob Agents Chemother. 2007; 51:1926–1933. [PubMed: 17371812]
55. Manary MJ, Singhakul SS, Flannery EL, Bopp SER, Corey VC, Bright AT, McNamara CW, Walker JR, Winzeler EA. Identification of pathogen genomic variants through an integrated pipeline. Bmc Bioinformatics. 2014; 15
56. DiCarlo JE, Norville JE, Mali P, Rios X, Aach J, Church GM. Genome engineering in Saccharomyces cerevisiae using CRISPR-Cas systems. Nucleic Acids Res. 2013; 41:4336–4343. [PubMed: 23460208]
57. Schiestl RH, Gietz RD. High efficiency transformation of intact yeast cells using single stranded nucleic acids as a carrier. Curr Genet. 1989; 16:339–346. [PubMed: 2692852]

58. Kostylev M, Otwell AE, Richardson RE, Suzuki Y. Cloning Should Be Simple: Escherichia coli DH5alpha-Mediated Assembly of Multiple DNA Fragments with Short End Homologies. PLoS ONE. 2015; 10:e0137466. [PubMed: 26348330]
59. Vieira DF, Choi JY, Calvet CM, Siqueira-Neto JL, Johnston JB, Kellar D, Gut J, Cameron MD, McKerrow JH, Roush WR, Podust LM. Binding mode and potency of N-indolyloxopyridinyl-4-aminopropanyl-based inhibitors targeting Trypanosoma cruzi CYP51. J Med Chem. 2014; 57:10162–10175. [PubMed: 25393646]
60. von Wachenfeldt C, Richardson TH, Cosme J, Johnson EF. Microsomal P450 2C3 is expressed as a soluble dimer in Escherichia coli following modification of its N-terminus. Arch Biochem Biophys. 1997; 339:107–114. [PubMed: 9056240]
61. Chen CK, Doyle PS, Yermalitskaya LV, Mackey ZB, Ang KK, McKerrow JH, Podust LM. Trypanosoma cruzi CYP51 inhibitor derived from a Mycobacterium tuberculosis screen hit. PLoS Negl Trop Dis. 2009; 3:e372. [PubMed: 19190730]
62. Leslie AGW. Recent changes to the MOSFLM package for processing film and image plate data. Joint CCP4 + ESF-EAMCB News-letter on Protein Crystallography. 1992; 26
63. Holton J, Alber T. Automated protein crystal structure determination using ELVES. Proc. Natl. Acad. Sci. U. S. A. 2004; 101:1537–1542. [PubMed: 14752198]
64. Murshudov GN, Vagin AA, Dodson EJ. Refinement of macromolecular structures by the maximum-likelihood method. Acta Crystallogr D Biol Crystallogr. 1997; 53:240–255. [PubMed: 15299926]
65. Collaborative Computational Project, N. The CCP4 suite: programs for protein crystallography. Acta Crystallogr D Biol Crystallogr. 1994; 50:760–763. [PubMed: 15299374]
66. Monk BC, Tomasiak TM, Keniya MV, Huschmann FU, Tyndall JDA, O'Connell JD, Cannon RD, McDonald JG, Rodriguez A, Finer-Moore JS, Stroud RM. Architecture of a single membrane spanning cytochrome P450 suggests constraints that orient the catalytic domain relative to a bilayer. Proc. Natl. Acad. Sci. U. S. A. 2014; 111:3865–3870. [PubMed: 24613931]
67. Berman HM, Westbrook J, Feng Z, Gilliland G, Bhat TN, Weissig H, Shindyalov IN, Bourne PE. The Protein Data Bank. Nucleic Acids Res. 2000; 28:235–242. [PubMed: 10592235]
68. Olsson MHM, Sondergaard CR, Rostkowski M, Jensen JH. PROPKA3: Consistent Treatment of Internal and Surface Residues in Empirical pK(a) Predictions. J. Chem. Theory Comput. 2011; 7:525–537. [PubMed: 26596171]
69. Jorgensen WL, Maxwell DS, TiradoRives J. Development and testing of the OPLS all-atom force field on conformational energetics and properties of organic liquids. J. Am. Chem. Soc. 1996; 118:11225–11236.
70. Kaminski GA, Friesner RA, Tirado-Rives J, Jorgensen WL. Evaluation and reparametrization of the OPLS-AA force field for proteins via comparison with accurate quantum chemical calculations on peptides. J. Phys. Chem. B. 2001; 105:6474–6487.
71. Friesner RA, Banks JL, Murphy RB, Halgren TA, Klicic JJ, Mainz DT, Repasky MP, Knoll EH, Shelley M, Perry JK, Shaw DE, Francis P, Shenkin PS. Glide: a new approach for rapid, accurate docking and scoring. 1. Method and assessment of docking accuracy. J. Med. Chem. 2004; 47:1739–1749. [PubMed: 15027865]
72. Friesner RA, Murphy RB, Repasky MP, Frye LL, Greenwood JR, Halgren TA, Sanschagrin PC, Mainz DT. Extra precision glide: Docking and scoring incorporating a model of hydrophobic enclosure for protein-ligand complexes. J. Med. Chem. 2006; 49:6177–6196. [PubMed: 17034125]
73. Halgren TA, Murphy RB, Friesner RA, Beard HS, Frye LL, Pollard WT, Banks JL. Glide: a new approach for rapid, accurate docking and scoring. 2. Enrichment factors in database screening. J. Med. Chem. 2004; 47:1750–1759. [PubMed: 15027866]
74. Repasky MP, Shelley M, Friesner RA. Flexible ligand docking with Glide. Curr. Protoc. Bioinformatics. 2007 Chapter 8, Unit 8 12.
75. Schuster-Bockler B, Schultz J, Rahmann S. HMM Logos for visualization of protein families. Bmc Bioinformatics. 2004; 5:7. [PubMed: 14736340]
76. Onyewu C, Blankenship JR, Del Poeta M, Heitman J. Ergosterol biosynthesis inhibitors become fungicidal when combined with calcineurin inhibitors against Candida albicans, Candida glabrata, and Candida krusei. Antimicrob. Agents Chemother. 2003; 47:956–964. [PubMed: 12604527]

77. Sagatova AA, Keniya MV, Wilson RK, Monk BC, Tyndall JDA. Structural Insights into Binding of the Antifungal Drug Fluconazole to Saccharomyces cerevisiae Lanosterol 14 alpha-Demethylase. Antimicrob Agents Ch 59. 2015:4982–4989.

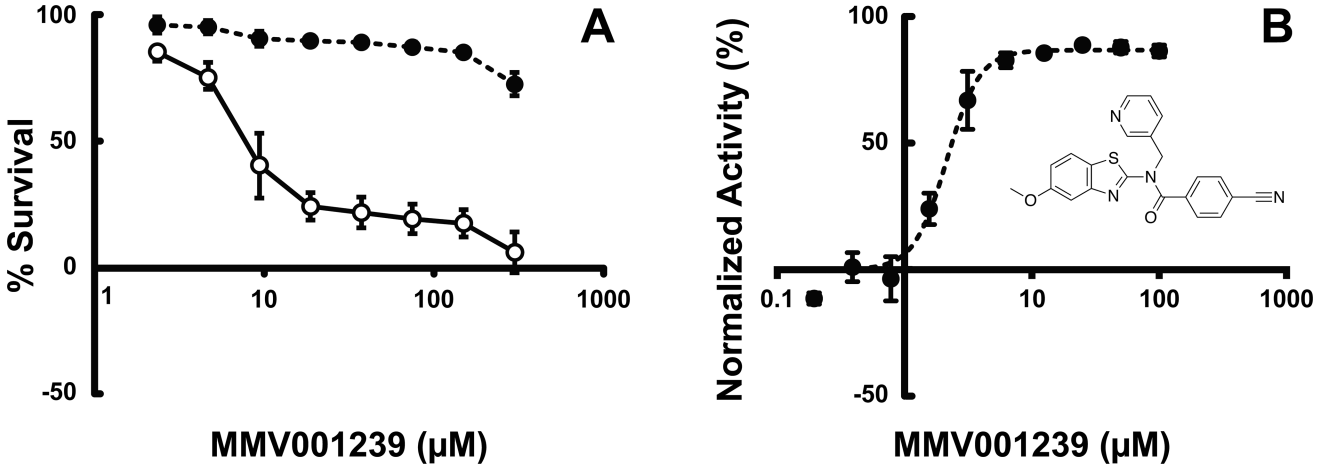


**Fig. 1. MMMV001239 activity against yeast and *T. cruzi***

A. MMV001239 dose-response curve for *S. cerevisiae*. Data points represent mean measurements taken from three independent 18 hour, 8-point dose response experiments. Error bars represent the standard error. The calculated average $IC_{50}$ concentration for the $ABC_{16}$-Monster strain (○) is 8.1 μM ± 1.2. For wild-type *S. cerevisiae* (●), no $IC_{50}$ value could be calculated because complete growth inhibition could not be achieved. B. MMV001239 activity against *T. cruzi* intracellular amastigotes. C2C12 myocytes were infected with *T. cruzi* trypomastigotes at a 15:1 parasite-to-host-cell ratio and treated with MMV001239 in varied concentrations. Compound activity was assessed after 72 h of treatment by determining the number of amastigotes per total host cells, normalizing to vehicle control and to positive control (uninfected cells).

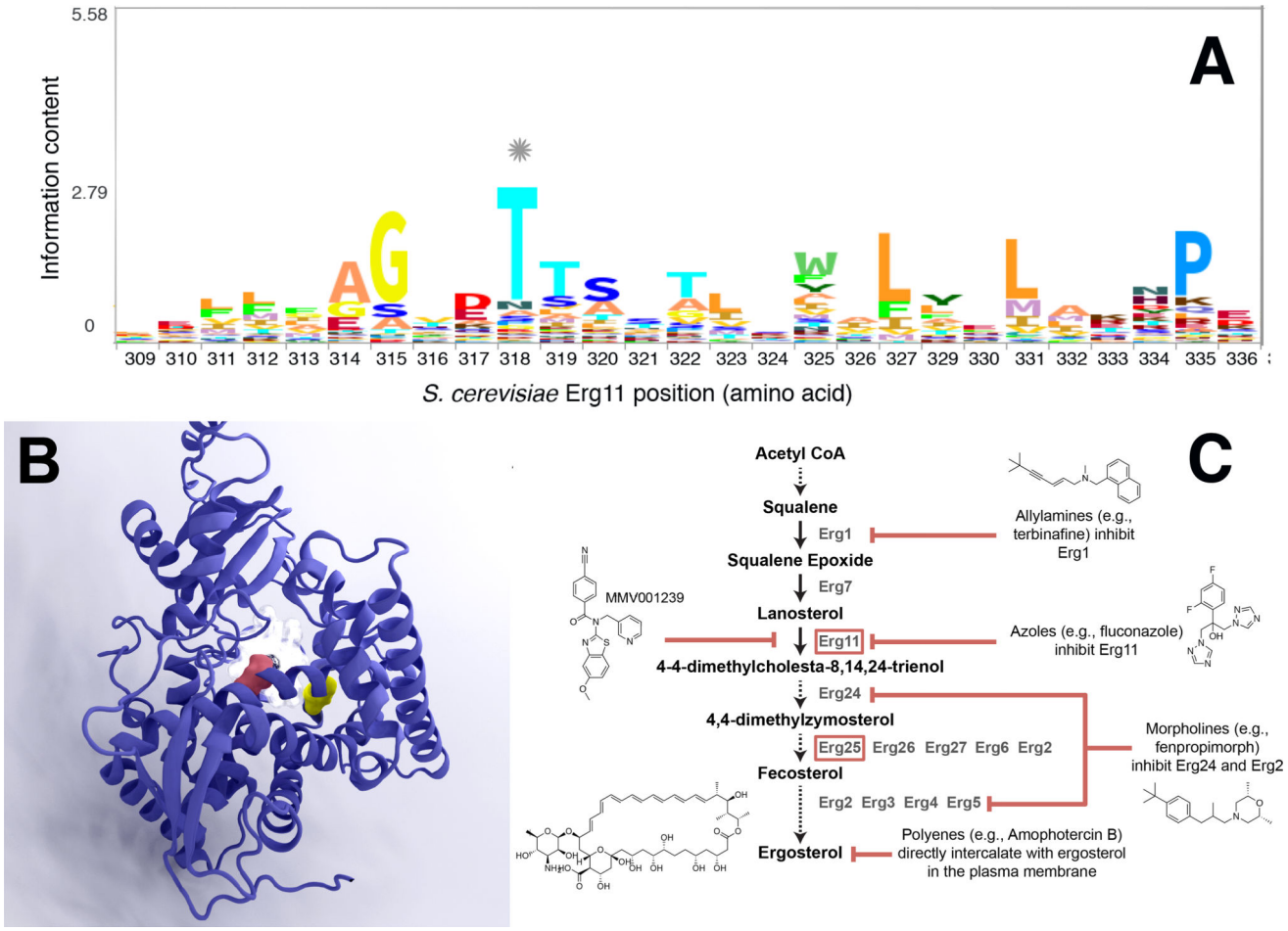


**Fig. 2. Characterization of MMV001239-resistant lineages obtained through directed evolution**

A) After multiple rounds of selections, the $IC_{50}$ value of each mutant lineage was determined. Average $IC_{50}$ values were calculated from three independent experiments done in triplicate. B and C) Cells of the parental strain as well as the four resistant lineages were streaked out on a YPD plate (B) or a plate containing 10 μM MMV001239 (C) and incubated for 3 days at 30°C. $ABC_{16}$, parental strain (GM); R1, lineage 1; R2, lineage 2; R4, lineage 4; R11, lineage 11.

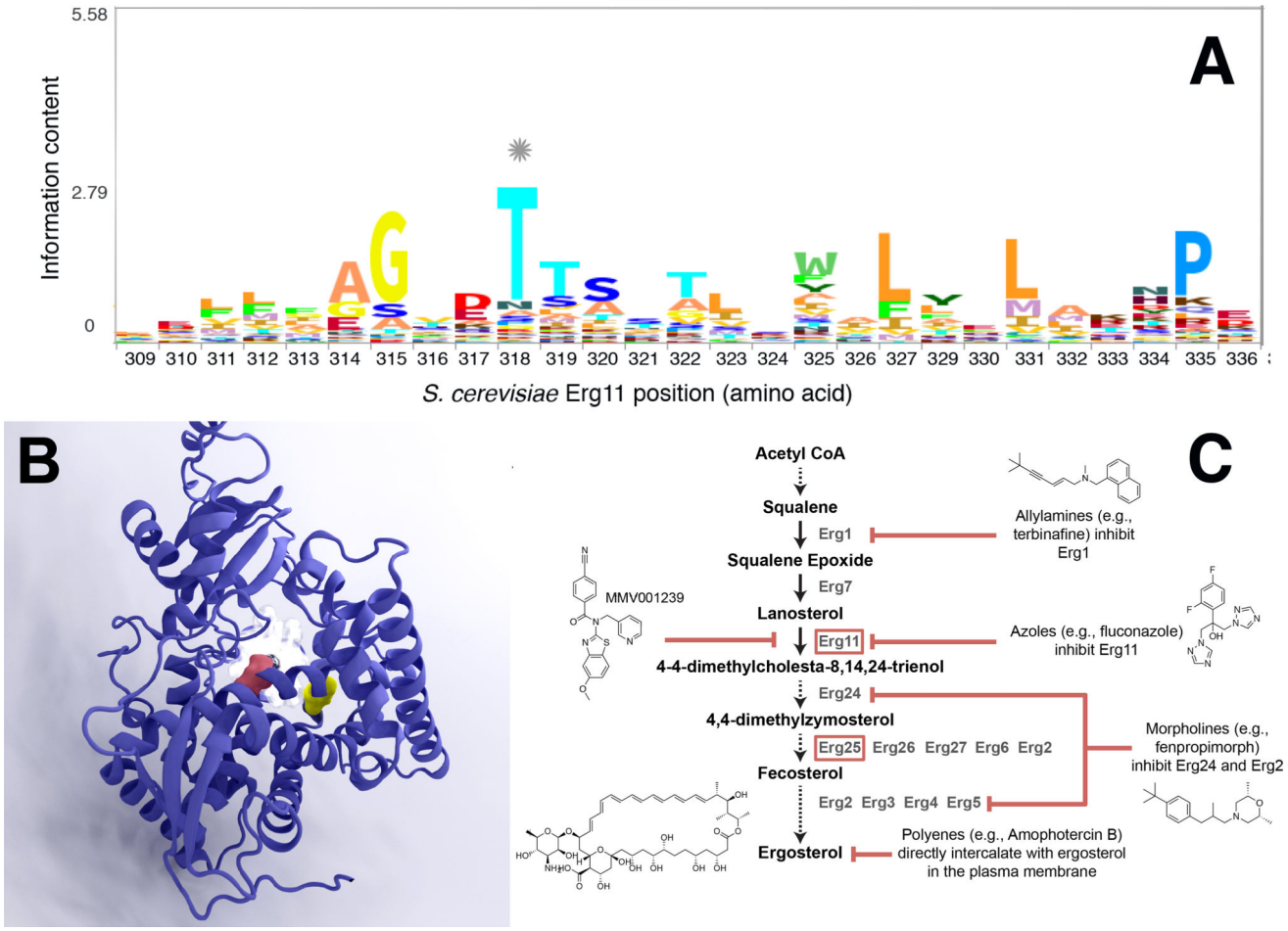


**Fig. 3. *ERG11* and the sterol biosynthesis pathway**

A. Sequence similarity of CYP51 proteins (pfam00067) is shown through a *profile Hidden Markov Model* (pHMM).[75] The highly conserved amino acid T318 that is mutated in lineage R2 is marked by an asterisk. B) CYP51 model (PDB ID 4K0F[66]). Residues shown as pink and yellow solid surfaces (T318 and V154, respectively) underwent directed-evolution-induced changes. Parts of the protein have been removed or otherwise modified to facilitate visualization. C). *S. cerevisiae* ergosterol biosynthesis pathway and associated drug classes. Figure adapted and modified from[76].

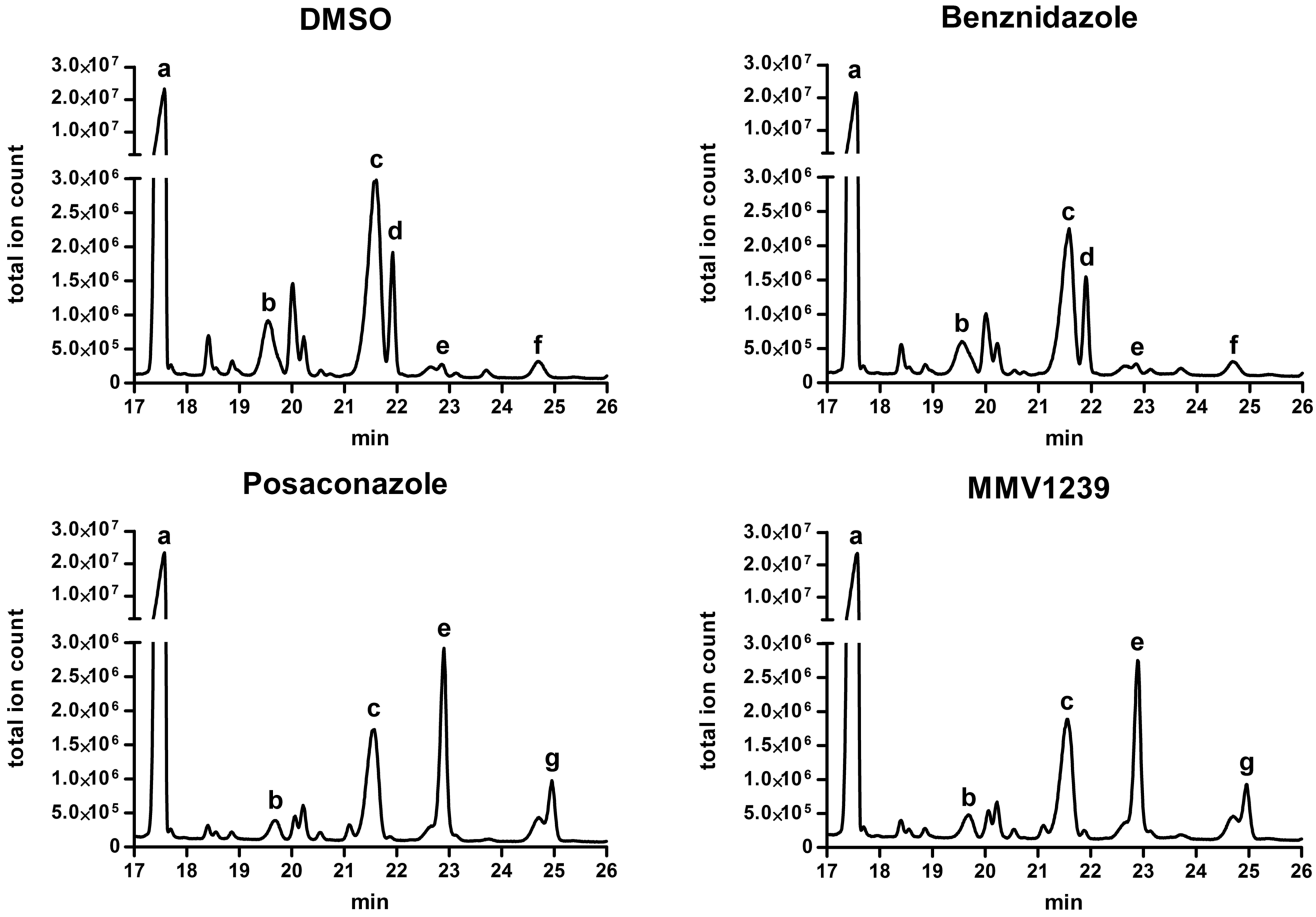


**Fig. 4. GC–MS sterol-profile analysis of intracellular *T. cruzi* amastigotes**

C2C12 myoblast cultures infected with *T. cruzi* show parasite-specific lipids corresponding to chromatographic peaks labeled as the following: (a) cholesterol originating from host cells, m/z = 458, tR = 17.3–17.7 min; (b) ergosterol, m/z = 468, tR = 19.3–19.8 min; (c) ergosta-7,24-diene-3-β-ol (episterol), m/z = 470, tR = 21.3–21.8 min; (d) ergosta-8,24-diene-3-β-ol (fecosterol), m/z = 470, tR = 21.7–22 min; (e) lanosterol, m/z 498, tR = 22.7–23 min; (f) 4-methylepisterol, m/z = 484, tR = 24.4–24.9 min; (g) eburicol, m/z = 512, tR = 24.8–25.1 min. DMSO (vehicle) and benznidazole (a reference drug for Chagas disease) were used as negative controls. Posaconazole, a potent Cyp51 inhibitor, was used as a positive control. Inhibition of *T. cruzi* Cyp51 by posaconazole and MMV001239 is demonstrated by the accumulation of lanosterol (e) and eburicol (g), and the decline of fecosterol (d).

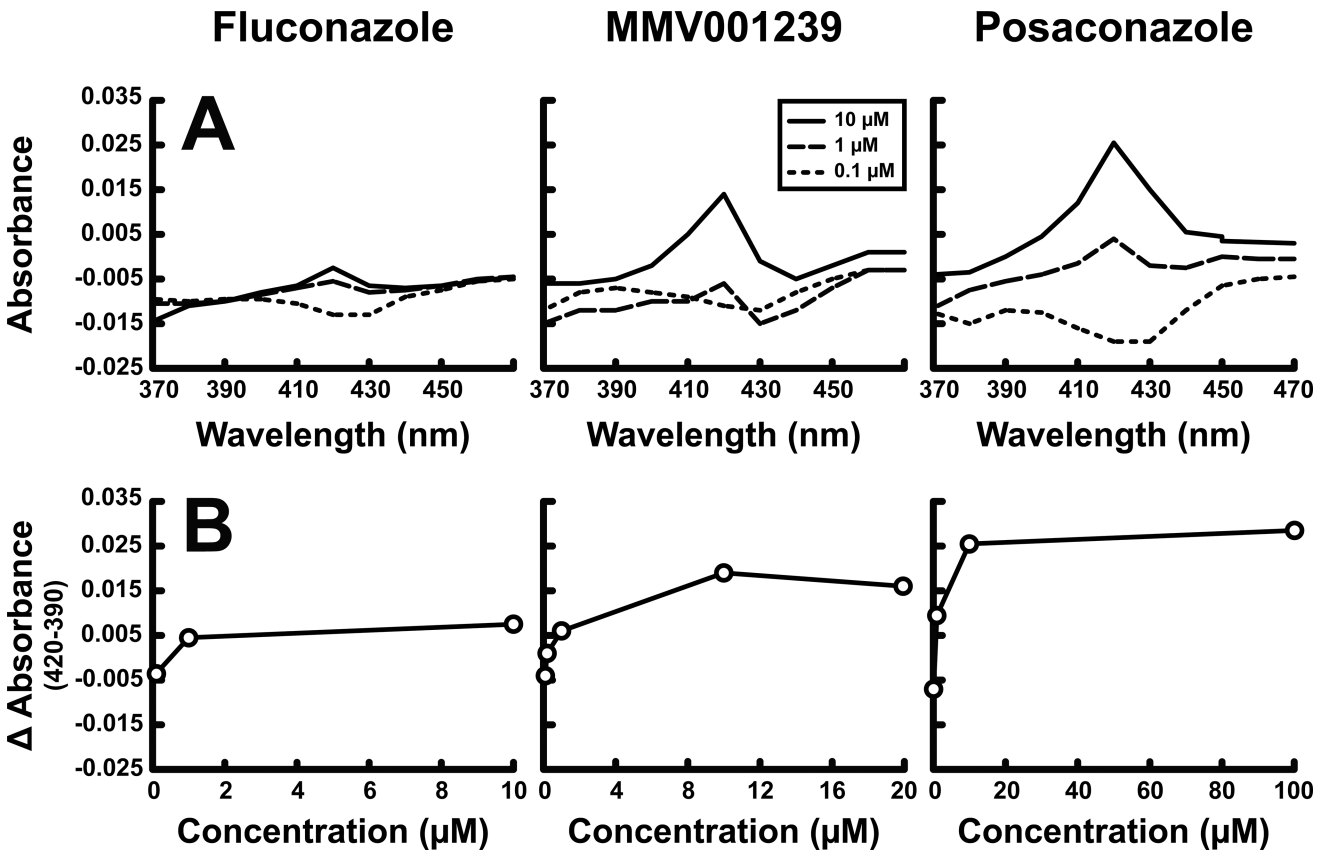


**Fig. 5. Determining binding potency with absorbance difference spectra**

A) To estimate the relative affinity of MMV001239 binding to *Tc*Cyp51, spectra were recorded across a range of compound concentrations. The MMV001239 spectra were compared to those of fluconazole and posaconazole, canonical weak and strong *Tc*Cyp51 inhibitors, respectively. B) Absorbance values at 390 were subtracted from those at 420 and plotted against inhibitor concentration. Relative potency can be determined from the maximum difference and the concentration at which it is reached.

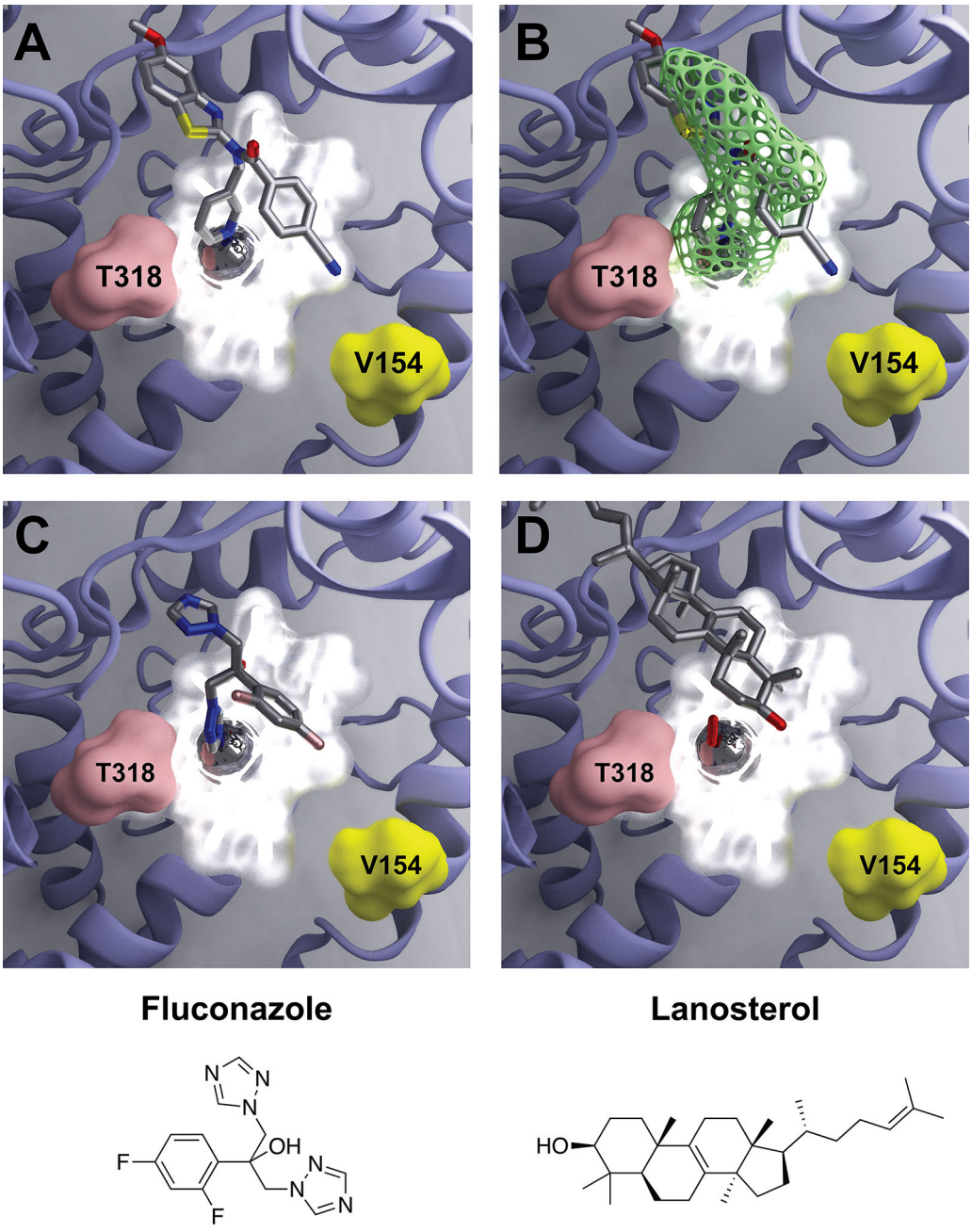


**Fig. 6. Small-molecule binding to *Sc*ERG11p**

A) MMV001239 was docked into CYP51 from *S. cerevisiae* (PDB ID 4K0F[66]). Residues that underwent directed-evolution-induced changes are shown as pink and yellow solid surfaces. Parts of the protein have been removed or otherwise modified to facilitate visualization. B) The MMV001239 docked pose into *Sc*ERG11p matched the low-resolution crystallographic density. The electron density (in green mesh) was visualized at an isovalue of 0.04. Most of the density was removed to facilitate visualization. C) The crystallographic pose of fluconazole, taken from the 4WMZ[77] structure, shown superimposed on 4K0F for reference. D) The crystallographic pose of lanosterol, taken from 4LXJ,[66] similarly

superimposed on 4K0F. Like MMV001239, these two well-characterized inhibitors also contain a nitrogenous heterocycle that interacts with the iron atom at the center of the heme group.

**Table 1**

**Results of whole-genome sequencing of the four resistant lines**

Resistance-conferring genes are indicated in bold. NSC, Nonsynonymous coding; SC, Synonymous coding; IG, intergenic. Common variants (Comm var) are defined as genes or intergenic mutations that have been repeatedly observed in other evolution studies. Trans, Retrotransposons. YMR045C and YBR012W-B encode Retrotransposon TYA Gag and TYB Pol genes.

| Lineage | Chr | Position | Codon | Effct | Impact | Amino Acid | Gene | Name | Comm Var |
|---|---|---|---|---|---|---|---|---|---|
| **MMV001239-R1-2** | I | 206144 | acC/acT | SC | SILENT | T914 | YAR050W | FLO1 | yes |
| | IV | 757631 | gcG/gcC | SC | SILENT | A668 | YDR150W | NUM1 | yes |
| | IV | 878244* | | IG | | | | | no |
| | VIII | 121223 | gTt/gGt | NSC | MISSENSE | V154G | YHR007C | **ERG11** | no |
| | XII | 734703 | | IG | | | | | yes |
| | XIII | 361550 | Cat/Tat | NSC | MISSENSE | H360Y | YMR045C | Trans. | yes |
| **MMV001239-R2-2** | I | 206144 | acC/acT | SC | SILENT | T914 | YAR050W | FLO1 | yes |
| | I | 25560 | acC/acT | SC | SILENT | T803 | YAL063C | FLO9 | yes |
| | IV | 757631 | gcG/gcC | SC | SILENT | A668 | YDR150W | NUM1 | yes |
| | VIII | 120731 | aCt/aAt | NSC | MISSENSE | T318N | YHR007C | **ERG11** | no |
| | X | 740238 | | IG | | | | | yes |
| | XII | 734703 | | IG | | | | | yes |
| | XIII | 361550 | Cat/Tat | NSC | MISSENSE | H360Y | YMR045C | Trans. | yes |
| **MMV001239-R4-2** | I | 206144 | acC/acT | SC | SILENT | T914 | YAR050W | FLO1 | yes |
| | I | 26412 | atC/atG | NSC | MISSENSE | I519M | YAL063C | FLO9 | yes |
| | VII | 611265 | gaC/gaA | NSC | MISSENSE | D234E | YGR060W | **ERG25** | no |
| | XII | 734703 | | IG | | | | | yes |
| | XIII | 361550 | Cat/Tat | NSC | MISSENSE | H360Y | YMR045C | Trans. | yes |
| **MMV001239-R11-2** | I | 206144 | acC/acT | SC | SILENT | T914 | YAR050W | FLO1 | yes |
| | II | 263153 | tCc/tTc | NSC | MISSENSE | S1095F | YBR012W-B | Trans. | yes |
| | IV | 757631 | gcG/gcC | SC | SILENT | A668 | YDR150W | NUM1 | yes |
| | VII | 611029 | Cat/Aat | NSC | MISSENSE | H156N | YGR060W | **ERG25** | no |
| | XII | 734703 | | IG | | | | | yes |

Author Manuscript

Author Manuscript

Author Manuscript

* located in the 3' utr of Ty-1 element

**Table 2**

***S. cerevisiae* susceptibility and dose-response data for MMV001239 resistant strains**

Compound $IC_{50}$ values for mutant *erg11 S. cerevisiae* strains selected by directed evolution (*erg11* R1 V154G and *erg11* R2 T318N), parental $ABC_{16}$-Monster strain (GM), and CRISPR/Cas9 engineered yeast (erg*11*:CRISPR V154G and *erg11*:CRISPR T318N). Experiments were performed in duplicates three or four independent times. SEM =Standard Error Measurement.

| Compound | GM $IC_{50}$ µM (SEM) | *erg11* R1 *V154G* $IC_{50}$ µM (SEM) | *erg11* R1 *T318N* $IC_{50}$ µM (SEM) | *erg11::V154G* CRISPR $IC_{50}$ µM (SEM) | *erg11::T318N* CRISPR $IC_{50}$ µM (SEM) |
|---|---|---|---|---|---|
| **MMV001239** | 14.49 (2.17) | 36.46 (5.75) | 59.09 (4.8) | 34.2 (5.77) | 54.54 (3.8) |
| **Cycloheximide** | 0.18 (0.03) | -- | -- | 0.16 (0.01) | 0.1 (0.01) |
| **Flucytosine** | 23.49 (4.82) | -- | -- | 31.89 (6.05) | 22.94 (1.73) |
| **Staurosporine** | 0.29 (0.11) | -- | -- | 0.33 (0.14) | 0.3 (0.11) |
| **Tavabarole** | 1.12 (0.05) | -- | -- | 1.04 (0.17) | 1 (0.17) |
| **KAE609** | 15.98 (0.56) | -- | -- | 16.58 (0.84) | 13.99 (0.65) |
| **Etoposide** | 48.29 (0.82) | -- | -- | 61.77 (13.91) | 32.93 (4.89) |